RESEARCH ARTICLE

The effect of flow speed and body size on Kármán gait kinematics in rainbow trout

Otar Akanyeti and James C. Liao*

The Whitney Laboratory for Marine Bioscience, Department of Biology, University of Florida, 9505 Ocean Shore Blvd, St Augustine, FL 32080-8610, USA

*Author for correspondence (jliao@whitney.ufl.edu)

SUMMARY

We have little understanding of how fish hold station in unsteady flows. Here, we investigated the effect of flow speed and body size on the kinematics of rainbow trout Kármán gaiting behind a 5 cm diameter cylinder. We established a set of criteria revealing that not all fish positioned in a vortex street are Kármán gaiting. By far the highest probability of Kármán gaiting occurred at intermediate flow speeds between 30 and 70 cm s^{-1}. We show that trout Kármán gait in a region of the cylinder wake where the velocity deficit is about 40% of the nominal flow. We observed that the relationships between certain kinematic and flow variables are largely preserved across flow speeds. Tail-beat frequency matched the measured vortex shedding frequency, which increased linearly with flow speed. Body wave speed was about 25% faster than the nominal flow velocity. At speeds where fish have a high probability of Kármán gaiting, body wavelength was about 25% longer than the cylinder wake wavelength. Likewise, the lateral (i.e. cross-stream) amplitude of the tail tip was about 50% greater than the expected lateral spacing of the cylinder vortices, while the body center amplitude was about 70% less. Lateral body center acceleration increased quadratically with speed. Head angle decreased with flow speed. While these values are different from those found in fish swimming in uniform flow, the strategy for locomotion is the same; fish adjust to increasing flow by increasing their tail-beat frequency. Body size also played a role in Kármán gaiting kinematics. Tail-beat amplitudes of Kármán gaiting increased with body size, as in freestream swimming, but were almost three times larger in magnitude. Larger fish had a shorter body wavelength and slower body wave speed than smaller fish, which is a surprising result compared with freestream swimming, where body wavelength and wave speed increased with size. In contrast to freestream swimming, tail-beat frequency for Kármán gaiting fish did not depend on body size and was a function of the vortex shedding frequency.

Key words: fish swimming, unsteady flow, vortex street, turbulence.

INTRODUCTION

Fish that live in moving water must contend with complex flows arising from current moving past objects. Understanding how fish swim in unsteady flows has attracted attention from many disciplines, ranging from stream ecologists investigating how fish relate to habitat, to engineers seeking the underlying principles of efficient propulsion (Streitlien and Triantafyllou, 1996; Heggenes, 2002; McMahon and Gordon, 1989; Triantafyllou et al., 2004; Pavlov et al., 2000). The hydrodynamics of a cylinder wake is rich in flow phenomena, as many studies demonstrate (for review, see Williamson, 1996). Examining how fish interact with vortices shed from a cylinder has provided a focused way to begin to understand how fish swim in unsteady flows (Webb, 1998; Liao et al., 2003a; Liao et al., 2003b; Sutterlin and Waddy, 1975). In particular, the ability to control the frequency and spacing of vortices by altering the flow speed and cylinder size, respectively, has provided a unique opportunity to study how fish behave in a complex yet predictable environment. Previous studies revealed that rainbow trout adopt novel body kinematics behind a cylinder, termed the Kármán gait, and pointed to common relationships between body kinematics and wake variables that were associated with energy savings (Liao et al., 2003a; Liao et al., 2003b; Liao, 2004; Taguchi and Liao, 2011). These studies largely concentrated on only one flow speed; we still know very little about how flow velocity influences the preference

and ability to Kármán gait. This represents a large gap in our understanding of how fish relate to unsteady flows because the vortex street is dynamically remodeled as flow speed increases (Zdravkovich, 1997). In addition, the effect of body size on Kármán gait kinematics remains unexplored.

In the absence of flow there is no vortex street associated with a cylinder. When water moves past a cylinder, shear layer instabilities around the cylinder give rise to regions of concentrated vorticity that grow and take turns inhibiting each other to cause the alternate shedding into the wake that forms a classic von Kármán vortex street (Williamson, 1996). Vortex shedding increases with flow speed, while the downstream–upstream spacing of the vortices remains the same, as it is dictated only by the cylinder diameter. A strong, stable low pressure region is also present on the lee side of the cylinder, where flow can move upstream, and which extends up to two cylinder diameter lengths downstream (Zdravkovich, 1997). As flow increases even more in this regime the vortex street gets stronger, resulting in lower pressures at each vortex center. The three-dimensional complexity of these vortices also increases with speed (Wei and Smith, 1986). The empirical interactions between these fluid phenomena and the flexible body of a fish are virtually unknown.

For undulatory locomotion in uniform flow (i.e. freestream swimming), the relationships between kinematic variables and

force generation have been established (Lighthill, 1971; Webb, 1992). As speed and size increase, body kinematics change predictably (Webb et al., 1984). In contrast, there are still fundamental questions that remain unanswered for fish swimming in a vortex street. What are the forces that a Kármán gaiting fish experiences as flow speed and body size increase, and how do body kinematics change to reflect the interactions with these forces? In order to establish a comprehensive understanding of Kármán gaiting, both of these questions need to be addressed. This study takes a crucial first step by characterizing the effects of flow speed and body size on the kinematics of trout swimming behind a cylinder.

MATERIALS AND METHODS
Animals
Rainbow trout, *Oncorhynchus mykiss* (Walbaum) were obtained from the Chattahoochee Forest National Fish Hatchery in Suches, GA, USA. Fish were held in a 473 l circular freshwater tank maintained at 15±1°C (DS-4-TXV Delta Star Chiller, Aqua Logic, San Diego, CA, USA) on a 12 h:12 h light:dark cycle and fed commercial trout pellets daily. Nine trout (L=15.7±0.8 cm, where L is total body length) were used for the experiments that investigated the effect of increasing flow velocity on Kármán gait kinematics. In another experiment, three size classes were selected. We chose the smallest size based on hatchery availability, and the largest size to avoid solid blocking effects given the dimensions of our flow tank. We categorized the sizes classes as small (L=10.4±0.1 cm, N=6 fish), medium (L=14.3±0.3 cm, N=6 fish) and large (L=18.6±0.6 cm, N=3 fish).

Experimental procedures
Trout were placed into a 175 l recirculating flow tank custom designed to hold a 5 cm diameter D-section cylinder in the working area (25×26×87 cm height×width×length), and allowed to acclimate to low flow for several minutes. A Phantom V12 video camera (Vision Research, Wayne, NJ, USA) was aimed at a 45 deg front-surface mirror placed below the flow tank and recorded the ventral view of the fish silhouetted against a light sheet for all flow speed experiments (Fig. 1). Video images (60 frames s^{-1}, 1280×800 pixels) were recorded for fish swimming behind the cylinder at flow speeds ranging from 10 to 90 cm s^{-1}, which corresponds to body-normalized swimming speeds of 1.0–6.0 L s^{-1}. Kármán gaiting kinematics across fish size were compared at a single, intermediate flow speed (~50 cm s^{-1}).

Cylinder parameters
Flow velocities were measured with a Höntzsch HFA flow probe (Waiblingen, Germany). Two Millar Mikro-Tip pressure transducers (Houston, TX, USA) on each side of the cylinder were used to directly measure the vortex shedding frequency across flow speeds. The vortex shedding frequency can also be predicted by the Strouhal equation:

$$St = \frac{fd}{U},\tag{1}$$

where St is Strouhal number, f is vortex shedding frequency, d is cylinder diameter and U is the nominal flow velocity. The Reynolds numbers for these experiments, calculated using a Strouhal number of 0.2 for bluff bodies, ranged between 5000 and 40,000 (Zdravkovich, 1997). We also measured the velocity deficit (i.e. the reduced velocity divided by the nominal velocity) at 5 cm intervals starting from behind the cylinder and extending 35 cm downstream.
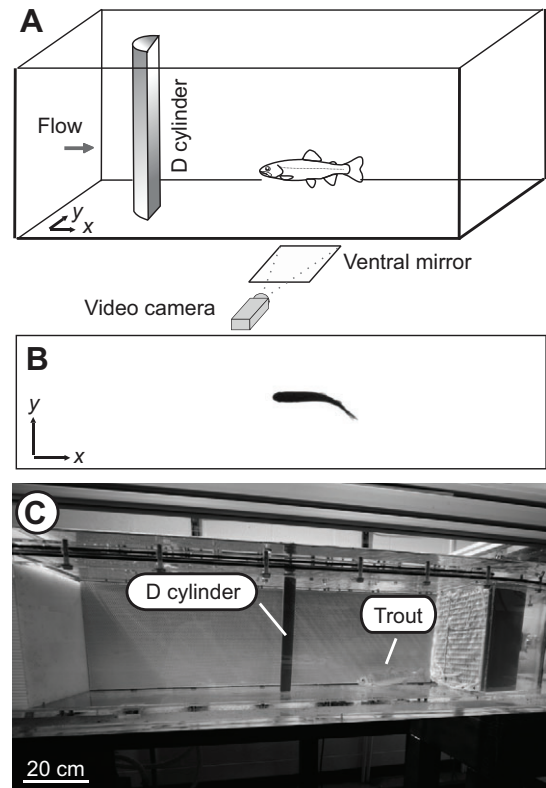

Fig. 1. Schematic diagram of the experimental setup. (A) Trout swam behind a stationary D-section cylinder positioned in a flow tank in which flow speed could be digitally controlled. A high-speed video camera was aimed at a front-surface mirror that was positioned under the flow tank at a 45 deg angle. (B) Ventral image of the fish in the flow tank. (C) Lateral view of the working section of the flow tank.

Cylinder wake wavelength describes the downstream–upstream spacing of vortices in a vortex street. Wake wavelength (0.2 m) was constant across speeds because it is dependent only on the cylinder diameter, and was calculated according to the equation:

$$\lambda = U/f.\tag{2}$$

Image analysis
The term Kármán gaiting was originally used to describe the behavior of a fish holding station in a vortex street for an extended period of time (Liao et al., 2003a). For the flow speed and body size selected for that study, Kármán gaiting fish displayed a large amplitude lateral translation and a decreased tail-beat frequency that was very different compared with when it was swimming in uniform flow.

For this study, we first selected video sequences based on the criterion that fish were holding station in the vortex street without drifting upstream or downstream. Video frames were captured for three to four tail-beat cycles for each fish and trial with 10 trials conducted for each flow speed. To identify videos in which fish were Kármán gaiting, we established the following five criteria: (1) the fish was holding station and did not drift upstream or downstream, (2) there was a traveling wave along the body, (3) the body displayed a large lateral displacement (>½L), (4) the body posture adopted a long wavelength (>1L), and (5) there were no transient small-amplitude, high-frequency tail beats. For the videos
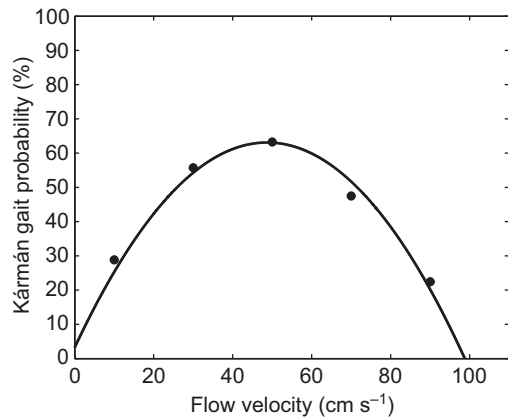
Fig. 2. The probability of Kármán gaiting changes with flow speed. Fish Kármán gait the most at intermediate flow speeds (~30–70 cm s⁻¹) and the least at extreme speeds. Videos were binned into five flow speed categories, where each category consisted of a minimum of 50 videos from at least five different fish.

that met these criteria, we performed two analyses. First, we estimated a probability function of Kármán gaiting by dividing the number of Kármán gait videos by the total number of videos. We use the term 'probability' to reflect the percentage of time that the fish was Kármán gaiting. Second, we analyzed how detailed Kármán gaiting kinematics changed across flow speed and body size.

A customized digitizing program (Matlab vR2009b) was used to mark points on each side of the body silhouette in the video images (Liao et al., 2003a). After a series of cubic spline functions were fitted to these points, a midline spline was constructed and then divided into 30 segments. The longitudinal positions of each segment were then recorded as relative body lengths.

Kármán gait kinematics

We measured the following variables: tail-beat frequency, body wave speed, body wavelength, lateral amplitude of the tail tip and body center (BC), lateral acceleration of the BC and maximum head angle. Tail-beat frequency was determined by averaging the number of tail-beat oscillations over a known time. Body wave speed was calculated by tracking the body crests moving from head to tail during Kármán gaiting. Body wavelength was derived from the body wave speed and tail-beat frequency using the relationship given in Eqn 2. Lateral amplitudes were measured as the maximum lateral excursion from the midline. BC refers to the center of mass of a dead fish, which was experimentally determined post-mortem for straight-stretched fish by iteratively moving bilateral pins down the body until we found the anteroposterior pin position for which the body balanced. We measured the distance of this point to the tip of the head. This distance was then used to determine a fixed point along the midline of each fish frame of the video. BC does not strictly refer to the actual center of mass, which can lie outside the body at times in freely swimming fish. Note that BC has been used to refer to the center of mass in previous work (Liao et al., 2003a; Liao, 2004). BC acceleration was calculated from the second derivative of BC lateral amplitude. To minimize error propagation, we first approximated the BC motion with a sine function as it oscillates with the vortex shedding frequency. We calculated the second derivative of the function and divided the amplitude by the square of the sampling interval. Head angle was calculated as the
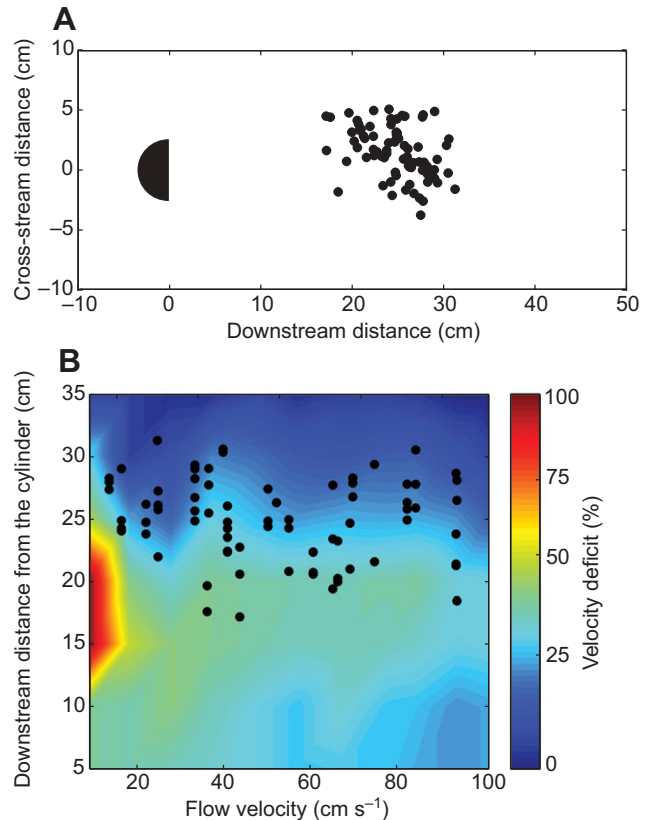

Fig. 3. (A) Location of the body center (BC, black circles) of the body relative to the D-cylinder for all trials. The x- and y-axes show the downstream and cross-stream position, respectively, where 0 corresponds to the cylinder axis. (B) Downstream position of the BC relative to the cylinder as flow velocity increases. The BC positions are superimposed on a heat map illustrating the magnitude of the velocity deficit behind the cylinder as a percentage of the freestream velocity, where red represents the greatest relative flow reduction. The location of greatest flow reduction remains in a consistent region downstream of the cylinder across most flow speeds. Note that this plot does not distinguish the reversal in flow direction that is established in the suction region directly behind the cylinder. At the lowest speed, flow reduction can equate to no flow (100% reduction), whereas at higher speeds the largest flow reduction still results in some flow magnitude.

standard deviation of the head angle relative to the axis of the freestream flow.

Analyses

All statistical analyses were performed in Matlab. We identified the relationship between kinematic variables and flow speed using linear regressions and evaluated the performance of the fit using r^2 values. We tested for significance at $P<0.05$. Certain kinematic variables (body amplitude, wavelength and BC acceleration) exhibited a non-linear dependence on increasing flow velocity. For body amplitude and wavelength, the relationship was linear at the slowest speeds, and then plateaued at higher speeds. To capture this relationship, we fitted the data with the equation:

$$y = Ax / (B + x), \qquad (1)$$

where the coefficients A and B were estimated using the least squares method. For BC acceleration, we used a second-order polynomial.

Kármán gaiting kinematic variables were compared with wake variables (i.e. vortex shedding frequency and wake wavelength)
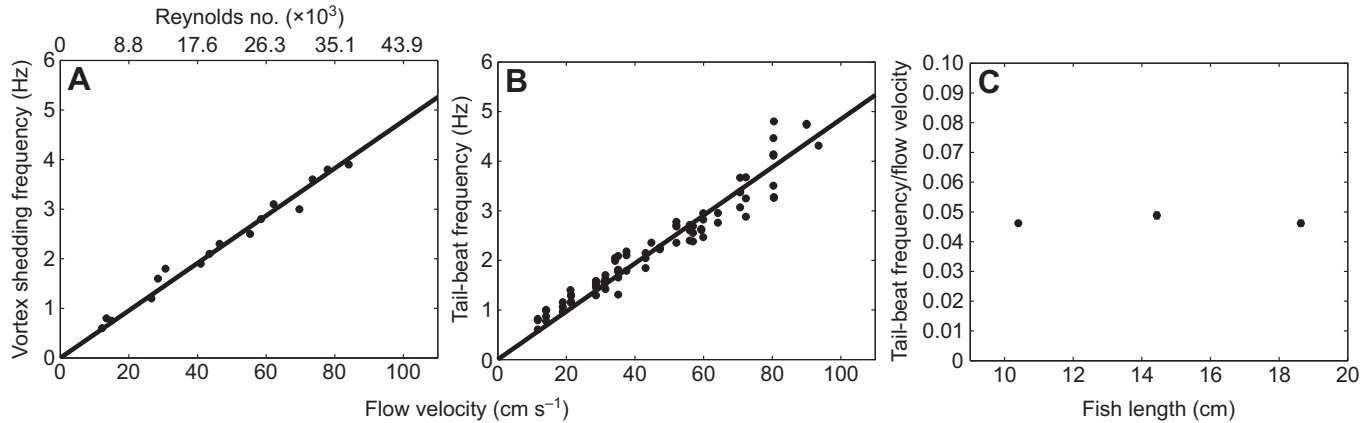
Fig. 4. Relationships between flow speed, vortex shedding frequency, tail-beat frequency and body size. (A) Experimentally measured vortex shedding frequency increases linearly with flow velocity (r^2=0.98, P<0.05). Reynolds number, using cylinder diameter as the length term, is shown at the top. (B) Tail-beat frequency for Kármán gaiting fish increases linearly and matches the vortex shedding frequency as flow velocity increases (r^2=0.93, P<0.05, N=9 fish). (C) Tail-beat frequency normalized to flow speed (~50 cm s^{-1}), showing no differences across body size (P=0.11, N=15 fish). Values shown are means ± s.e.m. Note that error bars are partially obscured by the data symbols.

at P<0.05. The values for kinematic variables were also compared with the values found for freestream swimming fish (Webb et al., 1984).

To analyze size effects on Kármán gait kinematics, one-way ANOVA were run on the individual kinematic variables (Bonferroni-corrected at P<0.05). To determine whether size groups were distinct from one another, we performed a principal component analysis (PCA) on all variables to reduce the dimensions of the parameter space. We then ran a MANOVA on principal component one (PC1) and principal component two (PC2) to see whether body size would explain the variance (P<0.05). The MANOVA took the simultaneous effects of all the kinematic variables into account, and thereby protected against a Type 1 error. All values are shown as the means ± s.e.m.

RESULTS

Not all fish that held station in the downstream wake of a cylinder were Kármán gaiting (i.e. met all five criteria). For fish positioned in the vortex street, the highest probability of Kármán gaiting (above 50%) occurred at intermediate flow speeds between ~30 and 70 cm s^{-1} (Fig. 2).

All fish positioned their bodies in a specific location relative to the cylinder. The BC of the fish was located about 4–6 cylinder diameters downstream from the cylinder for all velocity trials (Fig. 3A). The velocity deficit in this region was about 40% of the nominal velocity (Fig. 3B). The location of this 40% deficit region did not change relative to the cylinder across speeds. At the lowest speed, we observed almost no flow in a region 3–5 cylinder diameters behind the cylinder.

We next looked at the kinematic variables of Kármán gaiting fish and compared them with relevant hydrodynamic variables. The vortex shedding frequency of a cylinder was dependent on flow speed. Our measurements showed that it increased linearly with speed according to y=0.05x (Fig. 4A, r^2=0.98, P<0.05), similar to what is predicted by Eqn 1. Tail-beat frequency closely matched the vortex shedding frequency and increased with flow velocity according to y=0.05x (Fig. 4B, Table 1, r^2=0.93, P<0.05). There was no statistical difference between the slopes of the vortex shedding frequency and tail-beat frequency. For fish Kármán gaiting at a flow speed of ~50 cm s^{-1}, tail-beat frequency did not differ across the fish lengths used in this study (Fig. 4C).

Body wave speed increased with flow velocity as y=1.26x (Fig. 5A, r^2=0.85, P<0.05). The slope of the best fit line was greater for small fish than for medium or large fish (Fig. 5B, P<0.05). There was no difference between medium and large sized fish. This suggests that small fish control their body wave speed differently from large fish.

Flow speed affected the relationship between body wavelength and cylinder wavelength (Fig. 6A). At the lowest speed, body wavelength was shorter than cylinder wavelength. Body wavelength quickly rose above cylinder wavelength as flow increased above ~30 cm s^{-1}, according to:

$$y = 30.14x / (7.65 + x) \ (r^2 = 0.28). \tag{2}$$

At these speeds body wavelength was longer than the wake wavelength, similar to previous findings (Liao et al., 2003a). Small fish had a relatively longer body wavelength than medium or large fish (Fig. 6B, P<0.05). There was no difference in body wavelength between medium and large fish.

Table 1. The effect of body size on Kármán gait kinematics at ~50 cm s^{-1} flow

|	Small fish (10.4 cm)	Medium fish (14.4 cm)	Large fish (18.6 cm)
Tail-beat frequency (slope)	0.05±0.001	0.05±0.001	0.05±0.001
Body wavelength (cm)	34.88±1.35	24.86±0.86	28.22±1.26
Body wave speed (slope)	1.61±0.06	1.21±0.04	1.30±0.04
Tail-beat amplitude (cm)	6.44±0.25	7.93±0.30	8.63±0.61
BC amplitude (cm)	1.47±0.07	1.70±0.13	1.57±0.23
BC acceleration (cm s^{-2})	256.58±14.37	318.17±38.46	306.71±64.66
Head angle (deg)	6.32±0.42	7.77±0.52	8.93±0.66

BC, body center.
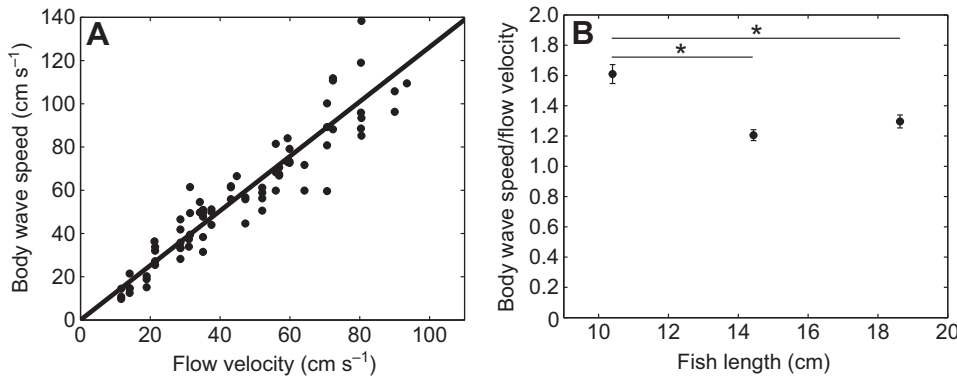
Fig. 5. Body wave speed is the product of tail-beat frequency and body wavelength, and increases with flow speed. (A) Body wave speed increases linearly with, and is 25% faster than, the nominal flow speed (r^2=0.85, P<0.05, N=9 fish). (B) At a flow speed of ~50 cm s^{-1}, small fish have a higher body wave speed than medium and large fish (*P<0.05, N=15 fish). Values shown are means ± s.e.m.

Lateral amplitude of the tail tip increased with flow velocity according to y=8.59x/(4.63+x) (Fig. 7A, r^2=0.14). At low speed, it was similar to the expected 5 cm lateral spacing of the vortices (as dictated by the cylinder diameter), but as flow speed increased it rose above this value and plateaued at ~7.5 cm. The lateral BC amplitude stayed relatively constant across speeds according to y=1.59x/(2.91+x) (r^2=0.07) and never exceeded the cylinder diameter value. Medium and large fish had a greater tail tip amplitude compared with small fish (Fig. 7B, P<0.05). There was no difference between medium and large sized fish. There was no effect of body size on BC amplitude.

The lateral acceleration of the BC increased quadratically with flow velocity according to y=0.14x^2+0.11x (Fig. 8A, r^2=0.69). Body size had no effect on BC acceleration (Fig. 8B).

Variation in head angle decreased with flow velocity according to y=−0.03x+9.47 (Fig. 9A, r^2=0.13, P<0.05). There is no difference between the average head angle and the freestream flow axis. Large fish had a larger variation in head angle than small fish (Fig. 9B, P<0.05).

A principal components analysis showed that PC1 and PC2 accounted for 85% and 11% of the total variance, respectively (Fig. 10). The variable that loaded the highest on PC1 was body wavelength, while the variables that loaded the highest on PC2 were tail tip amplitude and head angle. A MANOVA run on PC1 and PC2 revealed a difference in group means (P<0.05). Small fish were different from medium and large fish along PC1 (Table 2, F=23.2256, P<0.05), while along PC2, there was no difference between groups (F=3.4710, P>0.05).

DISCUSSION

Distortion of uniform flow by a cylinder creates local regions that fish can exploit to hold station. Trout will bow wake in the front of the cylinder, entrain to the side or Kármán gait in the vortex street downstream (Liao, 2007). Fish can also choose to avoid the cylinder and swim in uniform flow. Of these behaviors, Kármán gaiting is a particularly interesting way for fish to hold station because the ability to synchronize with drifting vortices translates into substantial energetic savings (Taguchi and Liao, 2011).

We found that the highest probability of Kármán gaiting occurred at intermediate speeds (Fig. 2). At low flow velocities, fish did not Kármán gait often and their motions resembled freestream swimming. This is because vortical flows must be sufficiently developed before fish can exploit them (Liao et al., 2003a; Liao et al., 2003b; Liao, 2004; Taguchi and Liao, 2011). Kinematic results support this interpretation; at a flow speed of 13 cm s^{-1} tail-beat frequency (2.5±0.2 Hz) was considerably higher than the vortex shedding frequency (0.7±0.2 Hz). Furthermore, tail-beat frequency at the low flow speed was identical to that of a freestream swimming fish (2.5±0.1 Hz) (Webb et al., 1984). Additionally, body wavelength (1.1±0.2 cm) and tail-beat amplitude (0.12±0.03 cm) were very similar to those found in freestream swimming fish (0.9±0.4 cm and 0.18±0.05 cm, respectively) (Webb et al., 1984). At the highest speeds, trout did not hold station continuously and were either drawn upstream into the suction zone behind the cylinder or ejected laterally from the vortex street. Under these high flow conditions the wake can adopt complex, three-dimensional vortex dynamics such as braid vortices and other hydrodynamic instabilities (Wei and Smith, 1986).

Kármán gait kinematics change across speed

The position of the body in the vortex street is a key component of Kármán gaiting. We discovered that fish position is not correlated to an absolute flow speed, but instead to a region where the velocity deficit is about 40% of the nominal flow. The location of this region did not change relative to the location of the cylinder across flow speeds. Unlike freestream swimming, Kármán gaiting is less about generating thrust and more about producing drag at the appropriate
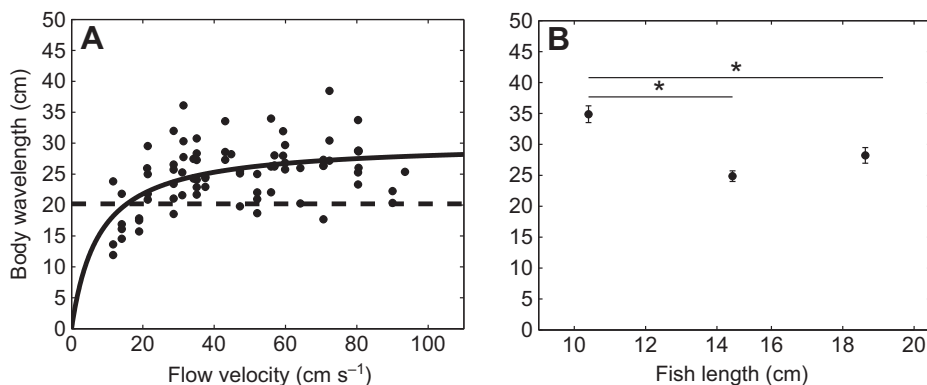

Fig. 6. Body wavelength across speed and body size. (A) Body wavelength (solid line) starts lower than the cylinder wake wavelength (dashed line) and then rises above it as flow speed increases (r^2=0.28, N=9 fish). At the lowest swimming speeds, the absence of a strong vortex street likely requires use of a shorter body wave similar to freestream swimming fish (see Discussion). (B) At a flow speed of ~50 cm s^{-1}, smaller fish have a longer body wavelength than larger fish (*P<0.05, N=15 fish). Values shown are means ± s.e.m.
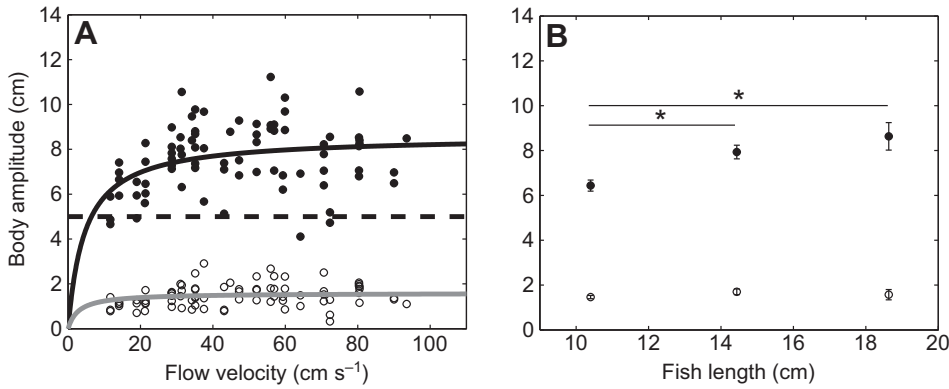
Fig. 7. Lateral body amplitude across speed and body size. (A) Tail tip amplitude (solid black line) is closest to the lateral vortex spacing defined by the cylinder diameter (dashed line) at the lowest speed and then rises above this as flow speed increases (r^2=0.14, N=9 fish). Lateral BC amplitude (gray line) is much smaller than both the tail tip amplitude and the lateral vortex spacing (r^2=0.07, N=9 fish). (B) At a flow speed of ~50 cm s^{-1}, tail tip amplitude increases with fish size except between medium and large fish (filled circles, *P<0.05, N=15 fish), unlike the BC amplitude (open circles, P=0.46, N=15 fish). Values shown are means ± s.e.m.

times to hold station (Liao et al., 2003a). Fish position themselves in a saddle point region. This region corresponds to a local minimum in the cross-stream direction, but seems to be unstable in the direction of the flow. Thus, if a fish approaches the cylinder too closely, it will be drawn into the suction zone. If a fish drifts too far downstream from where the vortex street is strongest, it will likely have to use active undulation. We found that this region starts about 20 cm downstream from the cylinder and encompasses approximately a 10 cm diameter area for this study.

In both freestream swimming and Kármán gaiting, fish responded to increasing flow speed by increasing body wave speed. To do so, fish increased tail-beat frequency while keeping body wavelength and amplitude constant. Why, in both behaviors, does tail-beat frequency change and not body wavelength? One hypothesis is that limitations in body flexibility or muscle physiology may prohibit fish from increasing relative body wavelength during a given behavior. Alternatively, under certain conditions, keeping body wavelength constant and increasing tail-beat frequency may be beneficial. For freestream swimming this seems like an appropriate strategy simply because of drag costs; passing small amplitude body waves faster is more efficient than passing large amplitude waves more slowly. However unlike in freestream swimming, a fish with a longer body wavelength in a vortex street may not necessarily experience more drag than a fish with a shorter body wavelength. We believe that Kármán gaiting is a flow-dominated behavior and that wake wavelength and vortex shedding frequency drive the body wavelength and tail-beat frequency. As the vortex shedding frequency, but not wavelength, increases with flow speed, it makes sense that body wavelength is preserved across flow speed. Most interestingly, these two behaviors occur in very different hydrodynamic environments yet still share the same control strategy; tail-beat frequency increases to compensate for increasing flow speed.

Experiments have shown that even a rigid foil positioned in a vortex street can generate thrust (Beal et al., 2006). What, then, is the role of the traveling wave in Kármán gait? In uniform flow, the ratio of the traveling wave to the forward body speed (i.e. slip) approaches unity when swimming is efficient because more momentum is directed towards forward thrust. This concept is less useful in a vortex street because we do not yet know how to evaluate efficiency for Kármán gaiting. In particular, what are the contributions of passive lift generation *versus* powered undulation in holding station? The traveling wave could simply be a physical consequence of a flexible body being buffeted by vortices. This seems unlikely given that across flow velocities body wave speed is consistently 25% greater in value than the speed of the drifting vortices (i.e. nominal flow speed). We anticipate additional advantages generated from the control of body posture and stiffness. This would require a simultaneous analysis of kinematics and visualization of vortex location with greater temporal resolution in future studies.

Our results suggest that the lateral acceleration of the body increased non-linearly because it was driven by steeper pressure gradients caused by vortex interactions as flow increased. We believe that the BC acceleration rises so sharply with speed because the pressure gradient across the flow follows a quadratic function, which in turn is due to the fact that the constant velocity deficit percentage across speed sets up a continuously increasing velocity gradient. Direct pressure measurements across the vortex street would confirm this hypothesis. This relationship is inherently unstable because acceleration cannot increase indefinitely with flow speed. We observed this at the highest flow speeds, where the probability of Kármán gaiting decreased substantially.

Large head angles increase drag in freestream swimming. For Kármán gaiting, we can envision two mechanisms for head control
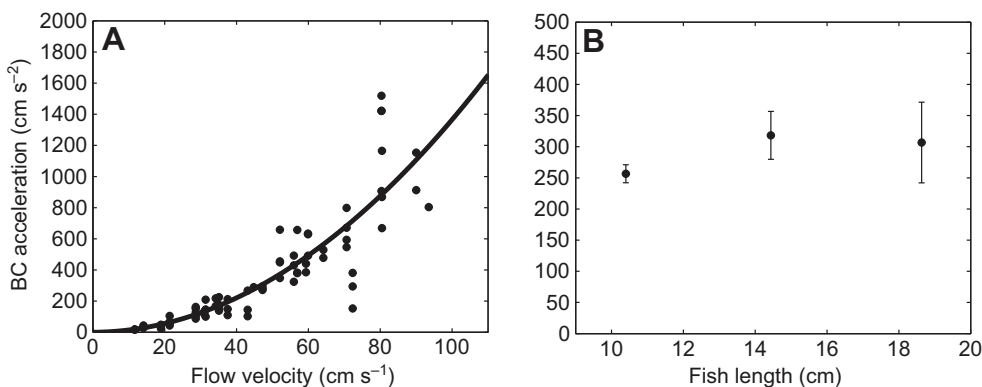

Fig. 8. Lateral acceleration of the BC across speed and body size. (A) BC acceleration increases quadratically with speed (r^2=0.69, N=9 fish). (B) There is no effect of body size on BC acceleration, although larger fish display more variation (P=0.51, N=15 fish). Values shown are means ± s.e.m.
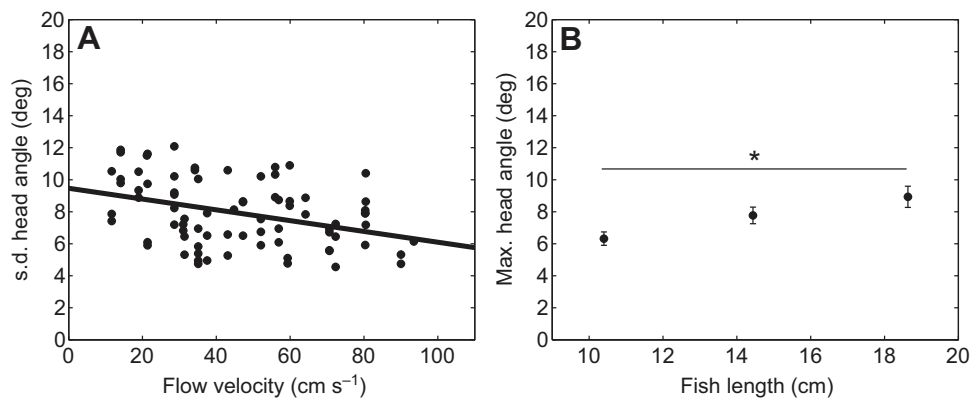
Fig. 9. Standard deviation of head angle from the axis of freestream flow across speed and body size. (A) Standard deviation of head angle decreases with flow velocity (r^2=0.13, $P<0.05$, N=9 fish). (B) At a flow speed of ~50 cm s^{-1}, the head angle deviation for large fish is greater than that for small fish ($P<0.05$, N=15 fish). Values shown are means ± s.e.m.

strategy, but ultimately more experiments are needed to understand which one is at play. The first mechanism assumes head angle is not under active control. In a high flow, high vortex shedding frequency situation, frequent interactions with vortices allow less time for the head to yaw at large angles. The second mechanism assumes that fish actively control their head angle. At lower flow speeds, fish have more time to respond to vortices, perhaps to increase stability. If this results in a higher head angle, the potentially greater drag may enable fish to stay in a favorable position in the vortex street. If at the highest flow speeds the drag caused by head angle were reduced, it may explain why we observed fish being drawn into the suction region more often.

Kármán gait kinematics at the lowest speeds

Kármán gaiting is different at lower flow speeds compared with higher speeds. At lower speeds, both body wavelength and tail tip amplitude are smaller than wake wavelength and cylinder diameter, respectively. When body wavelength is not greater than wake wavelength, this coincides with the fish having a lower probability of Kármán gaiting. This suggests that there is some specific relationship between body posture and vortices that facilitates station-holding, which is consistent with original observations (Liao et al., 2003a).

In this study, we found a linear increase in the vortex shedding frequency and assumed that the wake wavelength and lateral vortex spacing were constant across speed. However, these variables could
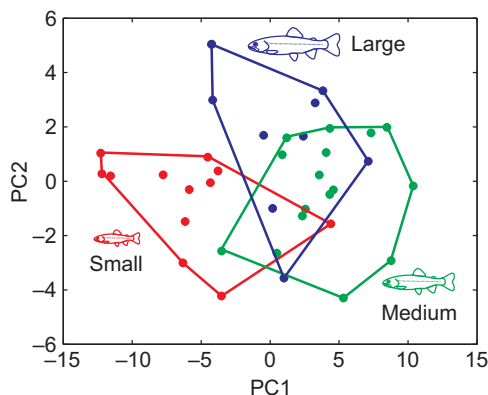

Fig. 10. Principal component analysis (PCA) of four Kármán gaiting kinematic variables on three body size treatments. PC1 and PC2 account for 85% and 11% of the variation, respectively. Small fish differ from medium and large fish only along PC1 ($P<0.05$, N=15 fish), in which the variable body wavelength loaded high. There is no difference between size groups along PC2 (P=0.08, N=15 fish).

change substantially if measured in the presence of a fish because of interactions between the fluid and the body.

Small fish Kármán gait differently

Fish relate to the vortex street in different ways depending on their body length. In the original description of the Kármán gait, two cylinders with diameters of 2.5 and 5.0 cm and one fish size (10 cm) were used to produce cylinder to body length ratios of 1:2 and 1:4 (Liao et al., 2003a). Here, we reveal that larger fish can also Kármán gait with cylinder to body length ratios of 1:2.8 and 1:3.7. Although these ratios are similar, they reflect two very different hydrodynamic environments. In the original study, the main objective was to see whether fish can control tail-beat frequency and body wavelength independently. This was done by using two different flow speeds and cylinder diameters in order to hold vortex shedding frequency constant while we changed wake wavelength, and *vice versa*. Compared with fish Kármán gaiting in the vortex street generated by a 2.5 cm diameter cylinder at 2.5Ls^{-1} (vortex shedding frequency=2.24±0.01 Hz, cylinder wake wavelength=1.12±0.01L), fish in the vortex street generated by a 5.0 cm diameter cylinder at 4.5Ls^{-1} (vortex shedding frequency=2.22±0.01 Hz, cylinder wake wavelength=2.03±0.01L) increased their body wavelength from 1.57±0.04L to 4.05±0.22L while maintaining a similar tail-beat frequency (~2.2 Hz). In addition, fish matched the two vortex shedding frequencies created by the 2.5 cm diameter cylinder at 2.5 and 4.5Ls^{-1} (vortex shedding frequency=2.24±0.01 and 4.02±0.02 Hz, respectively) while maintaining a constant body wavelength.

In contrast, one of the main objectives of this study was to investigate the effect of body size on Kármán gait kinematic variables. To do this, we kept vortex shedding frequency and wake wavelength constant by selecting only one cylinder size.

When small fish Kármán gait, they have a longer body wavelength than large fish. What is interesting is that in rainbow trout that are freestream swimming, body wavelength increases with size (Webb et al., 1984), but during Kármán gaiting the opposite is true. Using

Table 2. One-way ANOVA for Kármán gait kinematic variables

	d.f.	F	P
Tail-beat frequency	2	2.4034	0.1056
Body wavelength	2	22.1732	0.0001
Body wavespeed	2	20.5693	0.0001
Tail-beat amplitude	2	8.1708	0.0013
BC amplitude	2	0.7928	0.4608
BC acceleration	2	0.6850	0.5109
Head angle	2	5.1487	0.0111

Webb's freestream equation ($\lambda=1.43L^{0.83}$) the body wavelengths for small, medium and large size fish are 10.0, 13.0 and 16.2 cm, respectively. These values are still lower than those of Kármán gaiting, with the biggest difference seen for small fish. In freestream swimming, the increased flexural stiffness of larger fish due to the larger second moment of area would create a longer body wavelength. We believe that during the Kármán gait less of the body participates in the traveling wave. Therefore, a longer body length did not correspond to a longer body wavelength as it seems to do for freestream swimming.

In order to Kármán gait, small fish interacted with cylinder vortices differently than larger fish. The present study, along with the original study (Liao et al., 2003a), indicates that as the cylinder diameter to fish length ratio changes from 1:2 to 1:4 and the size of the vortices gets smaller relative to body length, the body wavelength decreases and approaches the cylinder wake wavelength. A longer body wavelength seems to be the result of increasing the relative size and spacing of the vortices. Hypothetically, a larger fish may be able to adopt a shorter wavelength because the body spans to interact with two successive vortices, while a smaller fish must adopt a longer, less sinuous wavelength because its body can only interact with one vortex. Put another way, a small vortex size relative to the body causes the fish to conform to the wake wavelength because local regions of the body are bent by the flow, whereas a larger vortex may barely bend the body.

Regardless of body size, Kármán gaiting fish had a body wavelength that was longer than the wake wavelength at intermediate flow speeds. This relationship seems crucial to hold station and likely orients the body to create more thrust-generating interactions with passing vortices.

The tail-beat amplitudes of freestream swimming fish increase with fish length according to $\alpha=0.36L^{0.74}$, where small, medium and large fish have values of 2.1, 2.6 and 3.1 cm, respectively (Webb et al., 1984). Tail-beat amplitude of Kármán gaiting fish also increases with fish size but these values are almost three times larger than the values of freestream swimming.

Fish size had no effect on tail-beat frequency, BC amplitude or acceleration. As the tail moved according to the encounter rate with shed vortices, the length of a fish should not prohibit it from synchronizing to the vortex shedding frequency. No change in BC amplitude suggests that the head and tail do not interact with vortices to amplify or constrict the lateral excursion of the body. The BC acceleration also does not change with fish size, presumably because larger forces resulting from greater surface area in larger fish are counteracted by a larger mass. We do see that larger fish show greater variation in their BC lateral acceleration, suggesting that they may be modifying their lateral motions by active control of their body and fins.

The hydrodynamics around a cylinder in flow are very rich in flow phenomena and provide a controlled environment to investigate the interactions between fish and unsteady flows. This study reveals new speed and size-related kinematic patterns for Kármán gaiting fish and substantially expands our understanding of how fish relate to vortices. As the ability to hold station depends specifically on how the body interacts with individual vortices in real time, comparisons of average values for kinematic variables and cylinder parameters cannot provide a complete understanding of Kármán gaiting. More detailed insights into the mechanisms of Kármán gaiting await simultaneous visualization of the flow and body kinematics on a cycle-by-cycle basis.

AUTHOR CONTRIBUTIONS

J.C.L. conceived and designed the research, and performed the experiments. O.A. and J.C.L. analyzed the data; interpreted the results of the experiments; prepared the figures; drafted, edited and revised the manuscript; and approved the final version of the manuscript.

COMPETING INTERESTS

No competing interests declared.

REFERENCES

Beal, D. N., Hover, F. S., Triantafyllou, M. S., Liao, J. C. and Lauder, G. V. (2006). Passive propulsion in vortex wakes. *J. Fluid Mech.* **549**, 385-402.

Heggenes, J. (2002). Flexible summer habitat selection by wild, allopatric brown trout in lotic environments. *Trans. Am. Fish. Soc.* **131**, 287-298.

Liao, J. C. (2004). Neuromuscular control of trout swimming in a vortex street: implications for energy economy during the Karman gait. *J. Exp. Biol.* **207**, 3495-3506.

Liao, J. C. (2007). A review of fish swimming mechanics and behaviour in altered flows. *Philos. Trans. R. Soc. B* **362**, 1973-1993.

Liao, J. C., Beal, D. N., Lauder, G. V. and Triantafyllou, M. S. (2003a). The Kármán gait: novel body kinematics of rainbow trout swimming in a vortex street. *J. Exp. Biol.* **206**, 1059-1073.

Liao, J. C., Beal, D. N., Lauder, G. V. and Triantafyllou, M. S. (2003b). Fish exploiting vortices decrease muscle activity. *Science* **302**, 1566-1569.

Lighthill, J. (1971). Large-amplitude elongated body theory of fish locomotion. *Proc. R. Soc. B* **179**, 125-138.

McMahon, T. E. and Gordon, F. H. (1989). Influence of cover complexity and current velocity on winter habitat use by juvenile coho salmon (*Oncorhynchus kisutch*). *Can. J. Fish. Aquat. Sci.* **46**, 1551-1557.

Pavlov, D. S., Lupandin, A. I. and Skorobogatov, M. A. (2000). The effects of flow turbulence on the behavior and distribution of fish. *J. Ichthyol.* **20**, S232-S261.

Streitlien, K. and Triantafyllou, G. S. (1996). Efficient foil propulsion through vortex control. *AIAA J.* **34**, 2315-2319.

Sutterlin, A. M. and Waddy, S. (1975). Possible role of the posterior lateral line in obstacle entrainment by brook trout (*Salvelinus fontinalis*). *J. Fish. Res. Board Can.* **32**, 2441-2446.

Taguchi, M. and Liao, J. C. (2011). Rainbow trout consume less oxygen in turbulence: the energetics of swimming behaviors at different speeds. *J. Exp. Biol.* **214**, 1428-1436.

Triantafyllou, M. S., Techet, A. H. and Hover, F. S. (2004). Review of experimental work in biomimetic foils. *IEEE J. Oceanic Eng.* **29**, 585-594.

Webb, P. W. (1992). Is the high cost of body/caudal fin undulatory swimming due to increased friction drag or inertial recoil? *J. Exp. Biol.* **162**, 157-166.

Webb, P. W. (1998). Entrainment by river chub nocomis micropogon and smallmouth bass micropterus dolomieu on cylinders. *J. Exp. Biol.* **201**, 2403-2412.

Webb, P. W., Kostecki, P. T. and Stevens, E. D. (1984). The effect of size and swimming speed on the locomotor kinematics of rainbow trout. *J. Exp. Biol.* **109**, 77-95.

Wei, T. and Smith, C. R. (1986). Secondary vortices in the wake of circular cylinders. *J. Fluid Mech.* **169**, 513-533.

Williamson, C. H. K. (1996). Vortex dynamics in the cylinder wake. *Annu. Rev. Fluid Mech.* **28**, 477-539.

Zdravkovich, M. M. (1997). *Flow Around Circular Cylinders: A Comprehensive Guide Through Flow Phenomena, Experiments, Applications, Mathematical Models, and Computer Simulations*. Oxford: Oxford University Press.